Personalized Medicine and Imaging

Clinical Cancer Research

ER$^+$ Breast Cancers Resistant to Prolonged Neoadjuvant Letrozole Exhibit an E2F4 Transcriptional Program Sensitive to CDK4/6 Inhibitors

Angel L. Guerrero-Zotano[1], Thomas P. Stricker[2], Luigi Formisano[1], Katherine E. Hutchinson[1], Daniel G. Stover[3], Kyung-Min Lee[1], Luis J. Schwarz[1], Jennifer M. Giltnane[2], Monica V. Estrada[4], Valerie M. Jansen[1], Alberto Servetto[1], Joaquín Gavilá[5], J. Alejandro Perez-Fidalgo[6], Ana Lluch[6], Antonio Llombart-Cussac[7], Mohamed Amine Bayar[8,9], Stefan Michiels[8,9], Fabrice André[10], Mónica Arnedos[10], Vicente Guillem[5], Amparo Ruiz-Simon[5], and Carlos L. Arteaga[1,4,11]

Downloaded from http://aacrjournals.org/clincancerres/article-pdf/24/11/2517/2045372/2517.pdf by KMLA - Hanyang University user on 23 June 2022

Abstract

Purpose: This study aimed to identify biomarkers of resistance to endocrine therapy in estrogen receptor–positive (ER$^+$) breast cancers treated with prolonged neoadjuvant letrozole.

Experimental Design: We performed targeted DNA and RNA sequencing in 68 ER$^+$ breast cancers from patients treated with preoperative letrozole (median, 7 months).

Results: Twenty-four tumors (35%) exhibited a PEPI score $\geq$4 and/or recurred after a median of 58 months and were considered endocrine resistant. Integration of the 47 most upregulated genes (log FC > 1, FDR < 0.03) in letrozole-resistant tumors with transcription-binding data showed significant overlap with 20 E2F4-regulated genes ($P = 2.56E{-}15$). In patients treated with the CDK4/6 inhibitor palbociclib before surgery, treatment significantly decreased expression of 24 of the 47 most upregulated genes in letrozole-resistant tumors, including 18 of the 20 E2F4 target genes. In long-term estrogen-deprived ER$^+$ breast cancer cells, palbociclib also downregulated all 20 E2F4 target genes and P-RB levels, whereas the ER downregulator fulvestrant or paclitaxel only partially suppressed expression of this set of genes and had no effect on P-RB. Finally, an E2F4 activation signature was strongly associated with resistance to aromatase inhibitors in the ACOSOG Z1031B neoadjuvant trial and with an increased risk of relapse in adjuvant-treated ER$^+$ tumors in METABRIC.

Conclusions: In tumors resistant to prolonged neoadjuvant letrozole, we identified a gene expression signature of E2F4 target activation. CDK4/6 inhibition suppressed E2F4 target gene expression in estrogen-deprived ER$^+$ breast cancer cells and in patients' ER$^+$ tumors, suggesting a potential benefit of adjuvant CDK4/6 inhibitors in patients with ER$^+$ breast cancer who fail to respond to preoperative estrogen deprivation. *Clin Cancer Res; 24(11); 2517–29. ©2018 AACR.*

[1]Departments of Medicine, Vanderbilt University Medical Center, Nashville, Tennessee. [2]Pathology, Microbiology & Immunology, Vanderbilt University Medical Center, Nashville, Tennessee. [3]Department of Medical Oncology, Dana-Farber Cancer Institute, Boston, Massachusetts. [4]Breast Cancer Program, Vanderbilt University Medical Center, Nashville, Tennessee. [5]Department of Medical Oncology, Instituto Valenciano de Oncología, Valencia, Spain. [6]Department of Oncology and Hematology, Hospital ClinicoUniversitario, INCLIVA Biomedical Research Institute, University of Valencia, CIBERONC, Valencia, Spain. [7]Department of Medical Oncology, Hospital Arnau de Vilanova, Valencia, Spain. [8]Service de Biostatistique et d'Epidémiologie, Gustave Roussy, Villejuif, France. [9]CESP, Faculté de Médecine, Université Paris Sud, Faculté de Médecine UVSQ, INSERM, Université Paris Saclay, Villejuif, France. [10]Department of Medical Oncology, Université Paris-Saclay, Gustave Roussy Cancer Campus, Villejuif, France. [11]Department of Cancer Biology, Vanderbilt-Ingram Cancer Center, Vanderbilt University Medical Center, Nashville, Tennessee.

Note: Supplementary data for this article are available at Clinical Cancer Research Online (http://clincancerres.aacrjournals.org/).

Corrected online January 10, 2019.

Corresponding Author: Carlos L. Arteaga, Vanderbilt University Medical Center, 2220 Pierce Avenue, 777 PRB, Nashville, TN 37232. Phone: 615-936-3524; Fax: 615-936-1790; E-mail: carlos.arteaga@utsouthwestern.edu

doi: 10.1158/1078-0432.CCR-17-2904

©2018 American Association for Cancer Research.

Introduction

Most breast cancers express estrogen receptors (ER$^+$) and are diagnosed in postmenopausal women (1). Therapeutic estrogen deprivation by use of aromatase inhibitors (AI) has been shown to reduce the risk of relapse and death after curative surgery (2). However, approximately 20% of patients with ER$^+$ breast cancer eventually relapse, suggesting mechanisms of *de novo* or acquired antiestrogen resistance to explain these recurrences (3).

Neoadjuvant trials with antiestrogens offer an opportunity to interrogate mechanisms of drug resistance that, in turn, could inform the choice of adjuvant therapy. Most of these neoadjuvant endocrine therapy studies have profiled pretreatment tumor biopsies to investigate genomic alterations associated with response. For example, Ellis and colleagues performed whole genome sequencing of 77 early breast cancers before treatment with neoadjuvant letrozole. This study revealed that *TP53* mutations are associated with drug resistance and that poorly responding tumors harbor more structural variations and mutations than sensitive tumors (4). However, profiling tumors after estrogen

Translational Relevance

Approximately 20% of patients with early ER$^+$ breast cancer treated with adjuvant antiestrogen therapy eventually relapse with metastatic disease. Herein, we show that those tumors enriched in E2F4 target genes following prolonged neoadjuvant estrogen deprivation with letrozole may benefit from adjuvant therapy with CDK4/6 inhibitors.

deprivation therapy instead of before treatment might be more clinically relevant, as it would integrate both the intrinsic biology of the tumor and the response to endocrine therapy. For example, three neoadjuvant trials (5–7) have shown that maintenance of a high tumor cell proliferation, as measured by Ki67 IHC in a biopsy obtained 2 weeks after treatment with an AI, is associated with an increased risk of cancer recurrence. Although some short-term presurgical studies have identified druggable alterations associated with drug resistance, defined as a high on treatment (~2-week) Ki67 score, only minor changes in variant allele frequency were detected between the baseline biopsy and drug-treated surgical specimen (8). This suggests the possibility that a short course of neoadjuvant endocrine therapy may only capture *de novo* mechanisms of antiestrogen resistance but fail to identify mechanisms of acquired resistance, such as the clonal expansion of drug-tolerant cells driven by resistant mutations and/or gene expression changes. Miller and colleagues (9) used whole genome sequencing and RNA sequencing (RNA-seq) in 22 ER$^+$ breast cancers before and after 4 months of estrogen deprivation with an AI showing significant temporal and spatial heterogeneity and a subclonal tumor composition that markedly changed upon treatment. Another study of gene expression of 18 matched pairs before and after 3 months of letrozole showed treatment-induced enrichment of cells with tumor-initiating and mesenchymal signatures (10). Taken together, these studies suggest that longer durations of therapy may be required to assess the full impact of AI-induced estrogen deprivation on the selection of drug-resistant populations.

We report herein a study where we performed targeted DNA sequencing and whole transcriptome analysis on whole tumor sections from a cohort of 68 operable ER$^+$ breast cancers treated with the aromatase inhibitor letrozole for a median of 7.2 months before surgery and a with a median follow up of 5 years. To define endocrine-resistant tumors, we used breast cancer relapse and the preoperative endocrine prognostic index (PEPI). This is a well-validated independent prognostic factor in the setting of neoadjuvant endocrine therapy that evaluates posttreatment ER levels, Ki67 score, tumor size, and axillary lymph nodal status (11). By incorporating data from treated surgical specimens rather than core biopsies, the PEPI score is less impacted by spatial intratumor heterogeneity (8) and may represent a strong surrogate of multiple drug-tolerant clonal populations.

Materials and Methods

Patients and tumor specimens

Tumors were from a cohort of newly diagnosed elderly patients with newly diagnosed, operable ER$^+$/HER$^-$ breast cancer treated with neoadjuvant letrozole at the Instituto Valenciano de Oncología in Valencia, Spain (12). Patients gave informed consent according to a protocol approved by the Instituto Valenciano de Oncología Institutional Review Board. They all underwent definitive surgery and had available tumor material for study endpoints. Patients were followed with serial ultrasound every 2 to 3 months during their preoperative treatment. Response to neoadjuvant therapy was annotated according to RECIST response criteria (13). Tumor specimens were promptly fixed after acquisition in 10% neutral-buffered formalin for 18 to 24 hours and embedded in paraffin. IHC was conducted in formalin-fixed, paraffin-embedded (FFPE) tumor blocks from both the diagnostic biopsy and the posttreatment whole surgical specimen. Tumor sections were subjected to IHC using Ki67 (Dako #M7240), ER (Santa Cruz Biotechnology #sc542), PR (Dako #M3569), and HER2 (Cell Signaling Technology #2242) antibodies according to methods reported elsewhere (14). FFPE tumor sections were scanned at ×100 magnification, and the area containing the highest number of Ki67$^+$ cells was selected. Positive and negative tumor cells were manually counted at 400×; the percentage of positive cells was calculated with at least 1,000 viable cells. Ki67 IHC was scored by two independent expert breast pathologists (M.V. Estrada and J.M. Giltnane). Patients were assigned a score according to the PEPI score (composite score of posttreatment ER, Ki67, T, and N status; ref. 11).

Statistical analysis

Comparisons between groups were performed using the *t* test for continuous variables and Fisher exact test for categorical variables. Time to breast cancer recurrence (BCR) was defined as the time from surgery to first local, regional, or distant disease recurrence. Patients without documented disease recurrence were censored at the date of their last disease evaluation. Time to BCR was estimated using the Kaplan–Meier method. Cox modeling was used to assess whether time to BCR differed with respect to PEPI status or E2F4 activation. All statistical tests were two sided, and differences were considered statistically significant when $P < 0.05$. FDR, used for correcting *P* values for multiple hypothesis testing, was computed using the Benjamini–Hochberg procedure. For gene expression analysis in Pre-Operative Palbociclib (POP) trial, we used an ANCOVA model to assess the effect of the treatment arms on the change from baseline to surgery. The covariates included in the model were the gene expression at baseline and the treatment arm. RT-PCR was performed in biological duplicate, and results are expressed as means ± SEM. R version 3.3.0 and GradPad prism version 6 were used for the statistical analyses and visual representations.

DNA and RNA extraction

DNA and RNA were extracted from four to eight 10-μm unstained whole FFPE tumor sections from surgical specimens (see Supplementary Methods).

DNA-targeted cancer gene sequencing

DNA alterations in 303 cancer-related genes using targeted exon capture by hybridization followed by next-generation sequencing were interrogated. Our custom design panel also included probes targeting common polymorphisms tiled throughout the genome to assist in identification of copy number

Downloaded from http://aacrjournals.org/clincancerres/article-pdf/24/11/2517/2045372/2517.pdf by KMLA - Hanyang University user on 23 June 2022

changes. Custom design was performed using the Nimblegen Nimble Design software (see Supplementary Methods).

Variant calling

To identify all variants in the samples, we used the GATK Haplotype Caller (15) for SNVs and indels. All reads with a mapping quality less than 70 were removed. Variants were annotated with ANNOVAR (16) using the genes' canonical transcripts as defined by Ensembl. Custom scripts were written to identify variants affecting splice sites using exon coordinates provided by Ensembl. Any spurious variant call with suspicious sequencing artifacts was removed. All SNVs and indels present in ExAC (17) with a population alternate allele frequency >0.1% that were not present in COSMIC were considered germline and subsequently removed. We also removed variants with allele frequency between 0.45 and 0.55, if not present in COSMIC. As a result, we obtained 330 nonsynonymous mutations in 153 genes. Mean depth of coverage across all samples was 319× (minimum, 25; maximum, 597; (Supplementary Fig. S2; Supplementary Table S7).

Driver and actionable mutations

To exclude possible passenger mutations, we selected all frameshift, nonsense and splice variants, and missense mutations and indels known or predicted to be damaging by at least 2 of 4 methods [SIFT (18), GERP++ (19), PolyPhen2 (20), OncodriveMUT (21)]. We classified variants as clinically actionable using www.cancergenomeinterpreter.org.

cDNA library preparation for RNA-seq

Total RNA was quantified using a Qubit (Life Technologies) and quality was assessed using an Agilent Bioanalyzer. For samples meeting quality requirements, 100 ng of RNA was used for library preparation following the manufacturer's protocol for Illumina RNA ACCESS (see Supplementary Methods).

RNA-seq data analysis

Detection of differentially expressed genes (DEG) between responder and nonresponder cases was performed with DESeq2 package (22), using raw RNA-seq counts as input. GO term enrichment analysis for DEGs was obtained using the online functional tool GSEA/MSigDB web site v6.1. We generated rlog-transformed count data using DESeq2, filtering low expressing genes (<5% tumors with 0 count and mean >4). This resulted in 16,730 transcripts that served as input for the following analysis: (i) single-sample gene set enrichment for 125 previously published breast cancer–related gene expression signatures calculated as described previously (23) and using a FDR <0.01, for differentially expressed signatures among subgroups; (ii) PAM50 molecular subtyping using R package genefu, using nonscaling option (24); (iii) sample-by-sample correlation matrix using Pearson distance of differentially expressed transcripts with the highest variance ($n = 256$), with the resulting matrix used to perform hierarchical cluster analysis by ward.D2; and (iv) statistical assessment of transcriptional diversity as described before (25). Gene expression data are provided in Supplementary Table S8.

The Cancer Genome Atlas, METABRIC, and ACOSOG Z1031B data

Somatic mutations, RNA-normalized gene expression, and clinical information for the breast-invasive breast carcinoma The Cancer Genome Atlas (TCGA) cohort (26) and METABRIC (27) were downloaded using the cBIO platform. ER^+ breast cancers were selected for comparison of somatic mutations (in TCGA) and PAM50 subtypes and survival (in METABRIC). Agilent gene expression arrays (GSE87411) were downloaded and used to compare E2F4 activation signatures between pretreatment and 2- to 4-week posttreatment samples from 109 patients' tumors in the ACOSOG Z1031B neoadjuvant trial (7).

Methods in POP trial

See Supplementary Methods for more information.

E2F4 activation signature

The E2F4 activation signature was generated by selecting those genes significantly upregulated (log fold change > 1, FDR < 0.03) in letrozole nonresponder versus responder tumors that were also significantly downregulated (FDR < 0.01) by a 14-day treatment with palbociclib in ER^+ tumors in the POP trial (NCT02008734). Eighteen of these genes are predicted to be E2F4 targets: *ANLN*, *ARHGAP11A*, *BUB1*, *CASC5*, *CDCA5*, *CDK1*, *CLSPN*, *DIAPH3*, *DTL*, *FAM111B*, *HIST1H3B*, *HIST1H3F*, *HMMR*, *KIAA1524*, *KIF18A*, *KIF4A*, *KPNA2*, *MAD2L1*, *PRR11*, *RRM2*, *STMN1*, *TICRR*, *TPX2*, and *ZNF367*. An E2F4 activation *Z*-score was developed by adding values across all genes for each tumor to generate an unescalated E2F4 score. The unescalated E2F4 score was then standardized to a *Z*-score by subtracting from each patient's score the mean score in the cohort, and then dividing it by the scores' SD.

Cell lines

MCF-7 cells and CAMA1 (from the ATCC, authenticated by the STR method) were maintained in Improved Modified Eagle Medium (IMEM)/10% FBS (Gibco). Long-term estrogen deprivation (LTED) cell lines were generated by culturing cells under hormone-depleted conditions [phenol red–free IMEM/10% dextran charcoal–treated FBS (DCC-FBS, HyClone; contains <0.0367 pmol/L 17β-estradiol)] as described previously (28). Mycoplasma testing was conducted before use. Experiments were performed less than 3 months after thawing early passage cells.

qRT-PCR

Cells were harvested, and their RNA was extracted using the RNeasy Mini Kit (QIAGEN Sciences Inc.). RNA (1 μg) was reverse transcribed to cDNA using the iScript cDNA Synthesis Kit [SuperScript III First-Strand (Invitrogen]. Real-time PCR reactions were conducted in 96-well plates using the iCycler iQ (Bio-Rad) and primers obtained from SABiosciences (Qiagen). Threshold cycle values were normalized for the housekeeping gene GAPDH. Specific primers for the genes of interest were designed using the tool NCBI/Primer-BLAST. The sequences of the primers set used for this analysis are listed in Supplementary Methods.

Immunoblot analysis

Cells were washed in PBS, harvested and lysed in NP-40 buffer [10 mmol/L Tris (pH 7.4), 1% NP-40, 150 mmol/L NaCl, 1 mmol/L EDTA, 1 mmol/L EGTA, 1 mmol/L sodium pyrophosphate, 50 mmol/L NaF, 10 nmol/L β-glycerophosphate, 5 mmol/L Na_3VO_4, 10% glycerol, 1 mmol/L PMSF, and protease inhibitors] for 10 minutes on ice. Protein concentrations

Downloaded from http://aacrjournals.org/clincancerres/article-pdf/24/11/2517/2045372/2517.pdf by KMLA - Hanyang University user on 23 June 2022

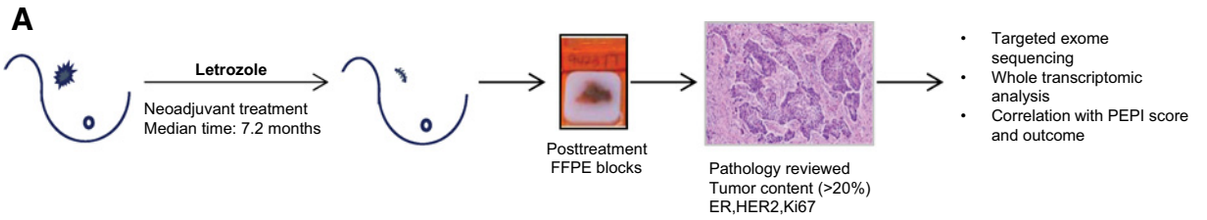

B

Characteristic	Patients No.	Patients %
Age, years		
60–70	6	8.8
70–80	46	67.6
>80	16	19.5
Tumor size, cm		
2–5	53	78
>5	15	22
Clinical stage		
Stage II	40	59
Stage III	28	41
Node status		
Negative	35	51.4
Positive	13	19.1
Unknown	20	29.4
Receptor status		
ER^+/PgR^+	45	66
ER^+/PgR^-	19	28
ER^-/PgR^+	4	6
HER2 status		
Negative	65	95.5
Positive	3	4.5
Ki67 (%)		
0–2	16	23.5
3–7	13	19.1
7–20	3	4.4
>20	27	39.7
Unknown	9	13.2
Histologic subtype		
Ductal carcinoma	47	69.1
Lobular carcinoma	13	19.1
Others	8	11.7

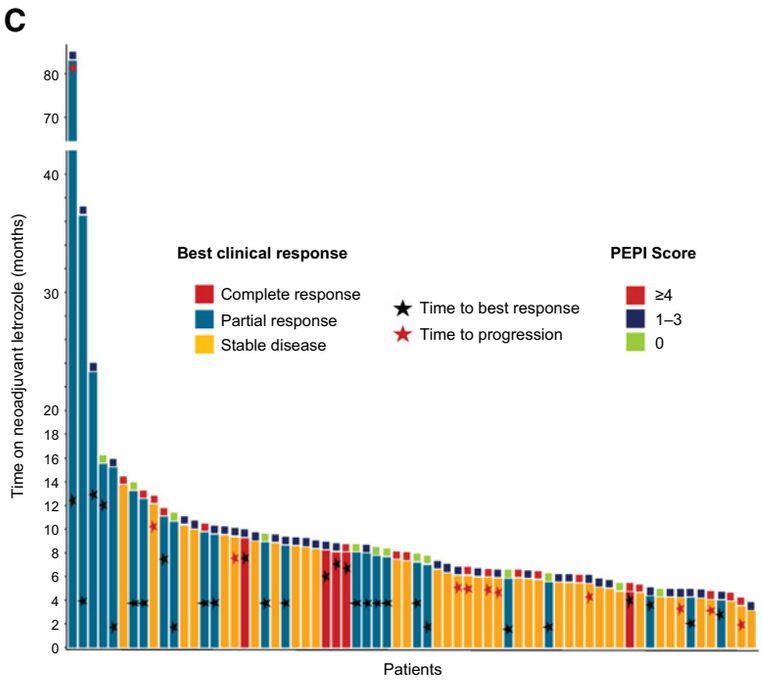

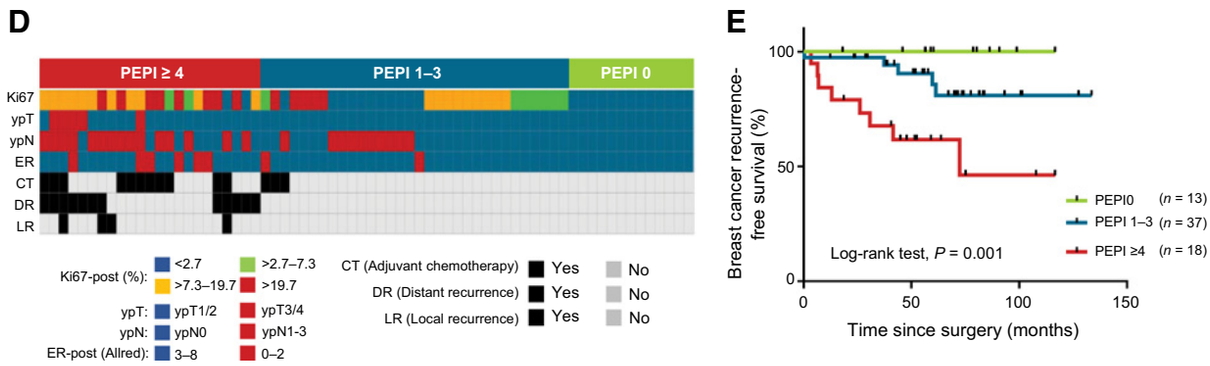

Figure 1.

PEPI score predicts long-term outcome after prolonged neoadjuvant letrozole. **A,** Study design. **B,** Patient characteristics. **C,** Individual patient response to prolonged neoadjuvant letrozole. Each bar represents a patient. The length of the bar shows duration of therapy; the color of the bar shows the best clinical response observed; stars mark the timing of the response; squares at the end of the bar show the PEPI score achieved. **D,** Each column represents a patient and its individual PEPI score assignment, adjuvant systemic treatment, and breast cancer events. **E,** Breast cancer recurrence-free survival by PEPI score.

of the lysates were determined by the BCA assay (Pierce Chemical Co.). Samples were separated by SDS-PAGE and transferred to PVDF membranes. Membranes were blocked with 3% nonfat dry milk in TBST for 1 hour at room temperature and then incubated overnight at 4°C with the appropriate primary antibody. Antibodies specific for RB (#9309; 1:1000), S780 P-RB (#9307; 1:1,000), and β-actin (#4970; 1:1,000) were obtained from Cell Signaling Technology; an ERα (#8002) antibody was from Santa Cruz Technology. Following incubation with horseradish peroxidase–conjugated secondary antibodies, proteins were visualized using an enhanced chemiluminescence detection system.

Downloaded from http://aacrjournals.org/clincancerres/article-pdf/24/11/2517/2045372/2517.pdf by KMLA - Hanyang University user on 23 June 2022

Data availability

The datasets generated during and/or analyzed during the current study are available from the corresponding author on reasonable request.

Results

PEPI score predicts long-term outcome after prolonged neoadjuvant letrozole

After informed consent, we treated 68 postmenopausal women with ER^+ operable breast cancer with neoadjuvant letrozole followed by surgery (Fig. 1A and B; Supplementary Fig. S1). Patients were treated for a median 7.2 months (interquartile range, 5.4–9.2). Median age was 77 years (range, 60–86); 40 (59%) had stage II and 28 (41%) had stage III cancer. Twenty-nine patients (42.5%) achieved a complete or partial response as measured by ultrasound; 10 experienced progressive disease within a mean of 5 months and underwent surgery. The median time to achieve a best objective response (complete or partial response) was 6.3 months (range, 2–16; Fig. 1C). After surgery, patients were classified according to their PEPI score (Supplementary Table S1; ref. 11). Thirteen (19%) patients had a PEPI score 0, 36 (52%) were PEPI 1–3, and 19 patients (28%) were PEPI $\geq$4. Adjuvant treatment consisted of endocrine therapy (96%), chemotherapy for 14 patients (20.5%) with high-risk features (10 with PEPI $\geq$4, 4 with PEPI 1–3), and radiotherapy (57%) for those patients who underwent breast-conserving surgery or mastectomy if the primary tumor was $\geq$4 cm or had $\geq$4 axillary lymph nodes involved with cancer (Fig. 1D). With a median follow-up of 58 months (range, 50–80), 13 patients (19%: 8 with PEPI $\geq$4, 5 with PEPI 1–3) exhibited a breast cancer recurrence (12 metastatic, 1 locoregional). The 5-year recurrence-free survival rate was 100%, 85% and 61% for PEPI 0, PEPI 1–3, and PEPI $\geq$4, respectively (log-rank test, $P = 0.001$; Fig. 1E). Patients with PEPI $\geq$4 continued to exhibit a poor prognosis after adjusting for adjuvant chemotherapy (risk of relapse for adjuvant chemotherapy, HR = 2.84, $P = 0.052$). The probability of achieving PEPI 0 correlated with a clinical response to neoadjuvant letrozole, with a response rate of 34% for PEPI 0 versus 5% for PEPI >0 ($P = 0.002$), but not to the length of neoadjuvant treatment (Supplementary Table S2).

Targeted gene sequencing identifies clinically actionable mutations in endocrine-resistant tumors

We performed targeted gene sequencing of 303 cancer-related genes, with a median depth of 320×. After applying a filtering algorithm (Supplementary Fig. S2), the median number of nonsynonymous somatic mutations per tumor was 4 (range, 0–46); in 5 tumors (3 PEPI 0, 2 PEPI 1–3), no somatic mutations were identified. There were 8 genes mutated in at least 5 patients: *PIK3CA* (40%), *CDH1* (21%), *KMT2C* (16%), *TP53* (14%), *NF1* (9%), *GATA3* (9%), *TBX3* (9%), and *MAP3K1* (9%; Fig. 2A). We detected only 1 ESR1 ligand-binding domain mutation, concordant with their low frequency in patients with progression on adjuvant AIs (29). Using an FDR <0.1, 12 genes were more frequently mutated in our cohort of residual tumors after long exposure to letrozole compared with untreated ER^+ breast cancer in TCGA. These genes are involved in transcriptional regulation (*MECOM*, *SETD2*, *SIN3A*, *STAG2*, and *PRDM1*), DNA repair (*POLE*, *PRKDC*), tumor suppression (*NF1*, *PHLPP1*), growth factor signaling (*ERBB4*, *IRS2*), and cytoskeleton remodeling (*EPKK1*; Fig. 2B). Using RNA-seq, data we assigned PAM50-intrinsic subtypes to each tumor and investigated subtype composition after prolonged estrogen deprivation with letrozole. As presented in Fig. 2C, the distribution of the intrinsic subtypes varied considerably compared with a cohort of untreated ER^+ breast cancers in the METABRIC database (27). There was an increase in cancers with basal-like and normal gene expression and a decrease in Luminal A tumors, suggesting treatment with letrozole remodeled the transcriptional landscape of these tumors. Tumors with basal/HER2–enriched gene expression were enriched among the letrozole-resistant tumors (9/15, or 56%, exhibited a PEPI score $\geq$4 and none had a PEPI score of 0).

We found 180 driver mutations in 99 genes (Supplementary Table S3A). Figure 2D shows the distribution of genes with 2 or more driver mutations (see Materials and Methods) according to PEPI score, PAM50 subtype, and patient outcome. Tumors were classified as nonresponder (PEPI $\geq$4 and/or recurrence) or responder (PEPI <4 and no recurrence). We could not find any statistically significant difference in the frequency of mutations or copy number alterations (CNA) between the two groups. However, the distribution of these alterations was asymmetrical with some mutations approaching overrepresentation in PEPI $\geq$4 versus PEPI 0 (*PIK3CA*: 50% vs. 10%, $P = 0.08$) and several alterations being absent in tumors with PEPI 0 (i.e., *TP53*, *AKT1*, *PTEN*, *ERBB2*). Other driver mutations, found to be more frequent in the letrozole-treated tumors in this cohort compared with those in TCGA (i.e., *NF1*, *STAG2*, *ERBB4*, *MECOM)*, were only detected in tumors with PEPI >0.

For CNAs, we focused on allelic imbalances (B-allele frequency > 3) in previously reported recurrently altered genomic regions. We detected 159 CNAs in 28 amplicons. These amplicons contained genes such as *CCND1* (16%), *FGFR1* (14%), *MYC* (10%), *ERBB2* (7%), or *ESR1* (5%). Amplicons with copy number loss included genes such as *KMT2C* (12%) and *PTEN* (3%). Thirty-nine CNA events in 9 genes were considered drivers (Supplementary Table S3B).

A total of 102 mutations in 48 driver genes and all driver CNAs were classified as clinically actionable (see Materials and Methods). Actionable mutations in the PI3K pathway *(PIK3CA*, *AKT1*, *TSC2*, and/or loss or truncation mutations of *PTEN)* were overrepresented in the PEPI $\geq$4 group compared with PEPI 0 (70% vs. 10%, $P = 0.003$). We also evaluated the association of each actionable mutation or CNA with the expression of a proliferation signature (PCNA), the intrinsic subtype, and the PEPI score. This allowed us to identify a subset of druggable somatic alterations (i.e., *NF1* loss, *TP53*, *NOTCH1*, *FGFR4*, *JAK1*, *PTPRD*) associated with multiple poor prognosis features (e.g., high PEPI, high PCNA score, and luminal B/HER2-enriched/basal subtypes), thus supporting the development of drugs targeting these alterations (Supplementary Fig. S3; Supplementary Table S3C and S4).

Endocrine-resistant tumors show enrichment in genes involved in proliferation through heterogeneous transcriptional and mutational profiles

We next performed comparative transcriptional analyses on 58 tumors. Analysis between responders and nonresponders showed 566 DEGs with an FDR <0.05, dominated by upregulated genes (458) in nonresponder versus responder tumors (Fig. 3A). Gene ontology enrichment analysis of DEGs showed that nonresponding tumors were enriched for cell cycle–related genes, while no overlap was found among responders (Fig. 3B).

Downloaded from http://aacrjournals.org/clincancerres/article-pdf/24/11/2517/2045372/2517.pdf by KMLA - Hanyang University user on 23 June 2022

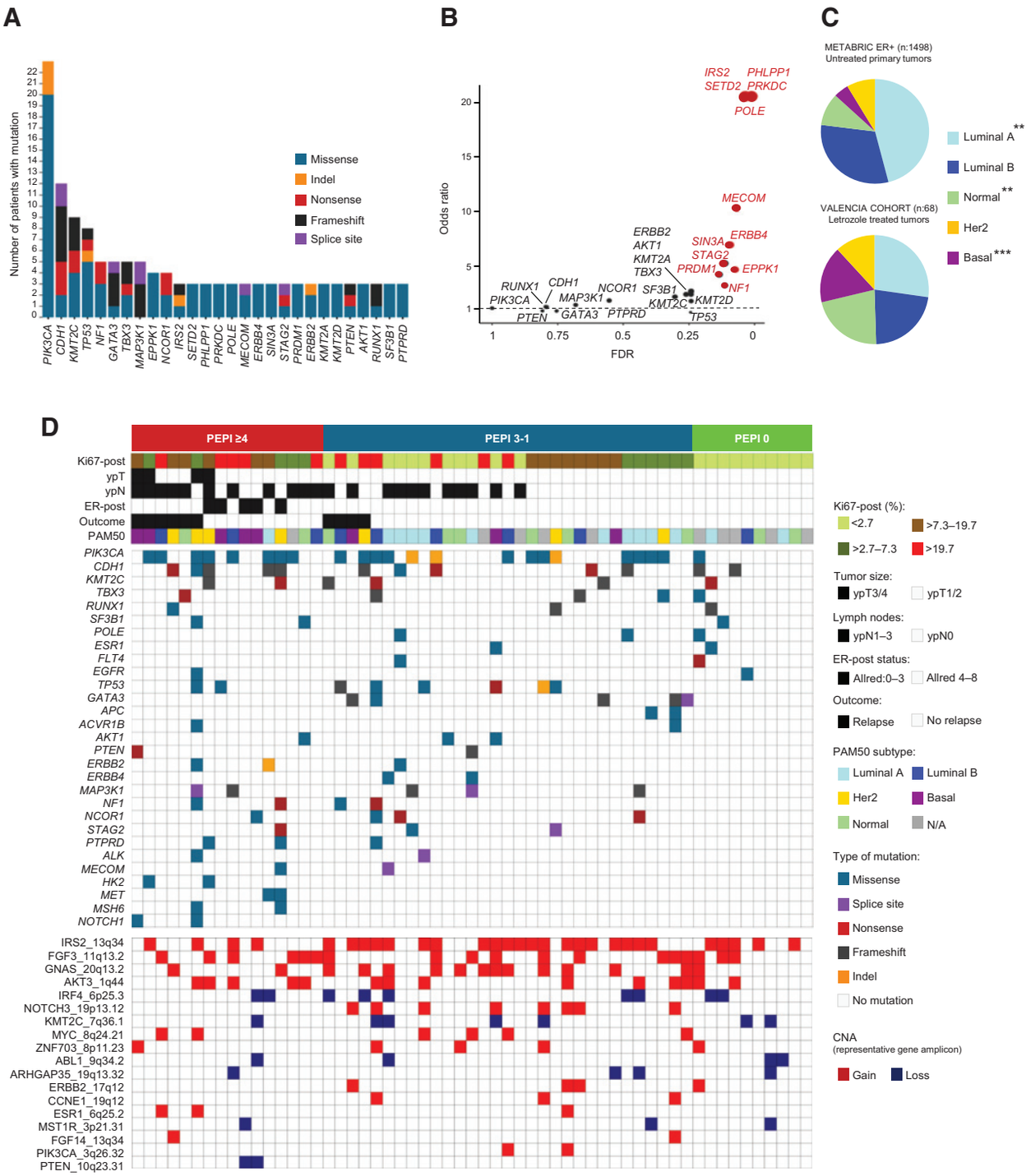

Figure 2.

Targeted exome sequencing identifies clinically actionable mutations and a unique distribution of breast cancer subtypes in endocrine-resistant tumors. **A,** Frequency and type of nonsynonymous recurrent gene mutations in 57 tumors from patients treated with neoadjuvant letrozole. **B,** Comparison of mutations detected in this cohort versus primary untreated ER$^+$ breast cancers in TCGA (Cell 2015; ref. 45); in red are genes with Fisher test FDR < 0.1. **C,** Distribution of PAM50-intrinsic subtypes in our cohort (Fig. 1) and in ER$^+$ early breast cancers from METABRIC (*P* value by Fisher test for the comparison among cohorts **, $P < 0.001$; ***, $P < 0.0001$). **D,** Tile plot showing the distribution of recurrent driver mutations ($n \geq 2$) and copy number alterations according to PEPI score and PAM50 subtypes; each column represents a patient.

Downloaded from http://aacrjournals.org/clincancerres/article-pdf/24/11/2517/2045372/2517.pdf by KMLA - Hanyang University user on 23 June 2022

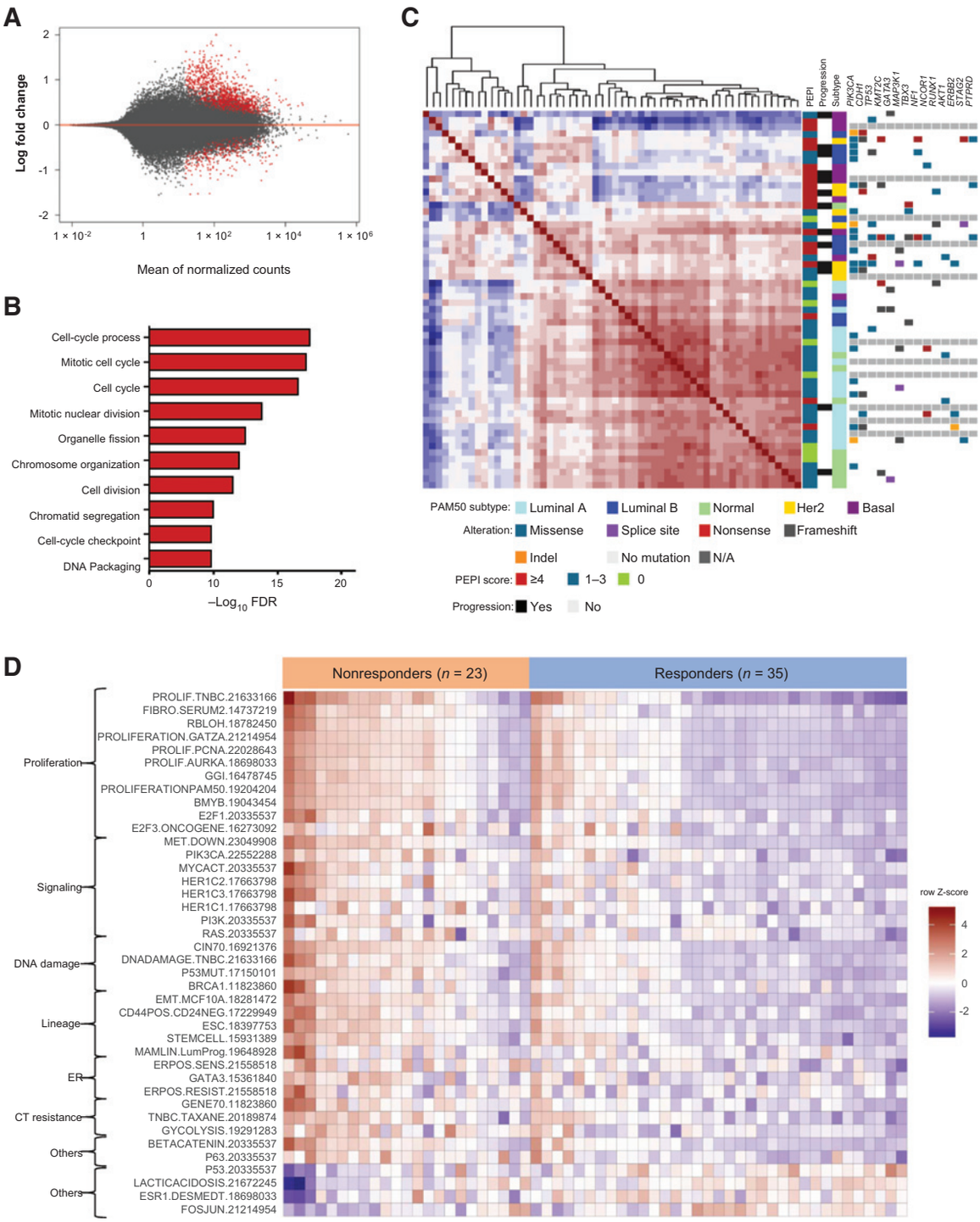

Figure 3.

Resistant tumors to letrozole show enrichment in cell cycle–related genes through a heterogeneous transcriptional and mutation profile. **A,** MA plot showing the $\log_2$ fold changes from nonresponders (PEPI $\geq$4 and/or breast cancer recurrence) over responder tumors (PEPI <4 and no breast cancer recurrence) of normalized counts (i.e., the average of counts normalized by size factor). Points in red represent normalized counts with an adjusted $P < 0.05$. **B,** GO enrichment of genes overexpressed in nonresponder tumors. **C,** Dendrogram and unsupervised clustered correlation matrix (red positive and blue negative correlation) of 58 breast cancers using Pearson distance. Differentially expressed genes between responders and nonresponder tumors were used to compute Pearson distance among the tumors and subsequent hierarchical clustering. Recurrent mutations, PEPI score, patient outcome, and PAM50 subtype are represented in columns in the right panel for each case. **D,** Single sample gene set enrichment analysis using a set of 125 breast cancer–related signatures shows differentially enrichment (FDR < 0.05) of 40 signatures between responder and nonresponder tumors.

Downloaded from http://aacrjournals.org/clincancerres/article-pdf/24/11/2517/2045372/2517.pdf by KMLA - Hanyang University user on 23 June 2022

To analyze the degree of variability among the tumors in their transcriptional response to estrogen deprivation with letrozole, DEGs between responders and nonresponders were used to perform a correlation matrix followed by unsupervised hierarchical clustering. This analysis revealed two main clusters: one relatively homogenous cluster integrating most of the responders and a second heterogeneous cluster enriched with nonresponders. Measurement of the transcriptional diversity showed a greater average distance to the median for the nonresponder compared with responding tumors (permutation test for homogeneity of multivariate dispersions <0.01). We also observed significant heterogeneity in somatic mutations between the two groups, with a greater mean number of mutations in nonresponders versus responders (12 vs. 3, $P < 0.0001$; Fig. 3C).

To investigate processes that are enriched in responders versus nonresponders, we analyzed differential signature enrichment using a set of 125 previously published breast cancer–related gene expression signatures (23). Thirty-six signatures were enriched in nonresponders and 4 in the responding tumors (FDR < 0.05). Endocrine-resistant tumors showed an enrichment of a diverse set of signatures involved cell cycle/proliferation, signaling pathway (EGFR1, PI3K, RAS), DNA repair, breast cancer stemness, ER signaling, and resistance to chemotherapy. Endocrine-sensitive tumors were enriched for signatures involved in p53 signaling, genes associated with ER expression, lactic acidosis response, and Fos–Jun kinase signaling (Fig. 3D). These results suggest some ER^+ breast cancers adapt to evade estradiol deprivation through different transcriptional programs that ultimately confer the ability of sustaining cell-cycle progression.

A CDK4/6 inhibitor–sensitive E2F4 transcriptional program is associated with estrogen-independent proliferation in letrozole-resistant tumors

To identify transcriptional programs with differential activity between sensitive and resistant tumors, we integrated transcription factor–binding data from chromatin immunoprecipitation sequencing (ChIP-seq) studies (CheA 2016 and ENCODE-TF ChIP-seq 2015) with expression of the 47 most upregulated genes in nonresponder tumors (log FC > 1, FDR < 0.03), using the platform Enrichr (30). E2F4 was the transcription factor whose targets demonstrated the most significant overlap with upregulated genes in the resistant list (overlap 20/710, adjusted $P = 2.56E{-}15$; Supplementary Table S5). E2F4 is repressed by binding to unphosphorylated Rb. Upon phosphorylation by a cyclin D/CDK4/6 complex, Rb is inactivated and uncoupled from E2F4, which, in turn, can induce transcription of genes associated with progression into the S-phase of the cell cycle and cell survival (31). Thus, we next tested whether the 20 E2F4-regulated genes were overexpressed in ER^+ breast cancer cells adapted to LTED, and whether they could be modulated by treatment with the CDK4/6 inhibitor palbociclib. We found upregulation of these genes in MCF7/LTED and CAMA1/LTED cells compared with parental MCF7 and CAMA1 cells, respectively (Fig. 4A). Treatment with palbociclib significantly downregulated the expression of all 20 E2F4-regulated genes (median decrease, 78%) with a simultaneous decrease in P-RB levels. Treatment with the ER downregulator fulvestrant or with paclitaxel only partially suppressed the expression of this set of genes and had no effect on P-RB levels (Fig. 4B–F).

Next, we investigated whether these genes could be modulated in primary breast cancers in patients enrolled in the POP trial (NCT02008734; ref. 32). In this study, patients with newly diagnosed, operable $ER^+/HER2^-$ breast cancer received palbociclib daily or placebo $\times 14$ days leading up to breast cancer surgery. Tumor cell proliferation and CDK4/6 inhibition were assessed by Ki67 IHC and P-RB IHC, respectively, in a pretreatment biopsy and in the (posttreatment) surgical specimen. Consistent with the inhibition of CDK4/6, treatment with palbociclib induced a significant reduction of P-RB levels and Ki67 (32). Next, we used gene expression array data from pre- and post-palbociclib tumors in this trial to assess expression of the 47 most upregulated genes in the tumors resistant to prolonged neoadjuvant letrozole (Fig. 1). Treatment with palbociclib, but not with placebo, significantly decreased expression of 24 of 47 of these resistance-associated genes (FDR < 0.01); among these were 18 of the 20 E2F4 target genes (Fig. 4G; Supplementary Table S6).

An E2F4 target gene signature is associated with resistance to neoadjuvant and adjuvant endocrine therapy

We generated a signature of E2F4 transcriptional activation, using the 24 genes associated with resistance to neoadjuvant letrozole and relapse in our cohort that were also significantly downregulated by palbociclib treatment in tumors in the POP trial, as compared with the placebo control group. We next assessed the ability of this set of genes to predict breast cancer recurrence in ER^+ treated with endocrine therapy. First, we tested the signature in the cohort of patients treated with prolonged neoadjuvant letrozole and showed that tumors within PEPI ≥ 4 had significantly higher E2F4 activation signature than tumors with PEPI 1–3 or PEPI 0 (Fig. 5A), and that E2F4 score was moderately correlated with posttreatment Ki67 levels (Fig. 5B). Furthermore, the 5-year relapse-free survival was 100%, 79%, and 45%, for patients in the low, medium, or high tertile of the E2F4 gene expression signature, respectively (log-rank test, $P = 0.0015$; Fig. 5C).

To externally validate the performance of the signature, we used gene expression data from patients treated with neoadjuvant AIs in the ACOSOG Z1031B study ($n = 110$; ref. 7). In this trial, tumors that failed to achieve a complete cell-cycle arrest (CCCA), defined as an on-treatment, 2-week Ki67 $\leq 2.7\%$, exhibited higher E2F4 signature score (Fig. 5D). Also, tumors with a high E2F4 score at baseline had a higher baseline Ki67 score and a worse response to AIs compared with those tumors with a low E2F4 score. CCCA rate was 18% versus 50% for high and low baseline E2F4 scores, respectively ($P < 0.001$; Fig. 5E). Of note, up to 40% of tumors with a high baseline E2F4 score switched to a low E2F4 score after 2-week treatment with an AI (Supplementary Fig. S4A). To assess the predictive value of the E2F4 activation signature in the adjuvant setting, we selected patients with ER^+ breast cancer treated with adjuvant endocrine therapy in the METABRIC cohort ($n = 1{,}408$). Patients with E2F4 scores in the higher tertile showed an increased risk of relapse [HR = 2.96; 95% confidence interval (CI), 2.176–3.670] and death (HR = 1.59; 95% CI, 1.32–1.94) compared with those in the lower tertile (Fig. 5F; Supplementary Fig. S4B). In addition, we evaluated luminal PAM50 subtypes and noted a significant association the E2F4 signature score with survival in both Luminal A and Luminal B breast cancer subtypes (Supplementary Fig. S4C and S4D).

Finally, we assessed the efficacy of palbociclib in tumors from patients in the POP trial. Treatment for 2 weeks with palbociclib suppressed Ki67 and P-RB levels' expression and downregulated all genes composing the signature (Fig. 5G). In the group of

Downloaded from http://aacrjournals.org/clincancerres/article-pdf/24/11/2517/2045372/2517.pdf by KMLA - Hanyang University user on 23 June 2022

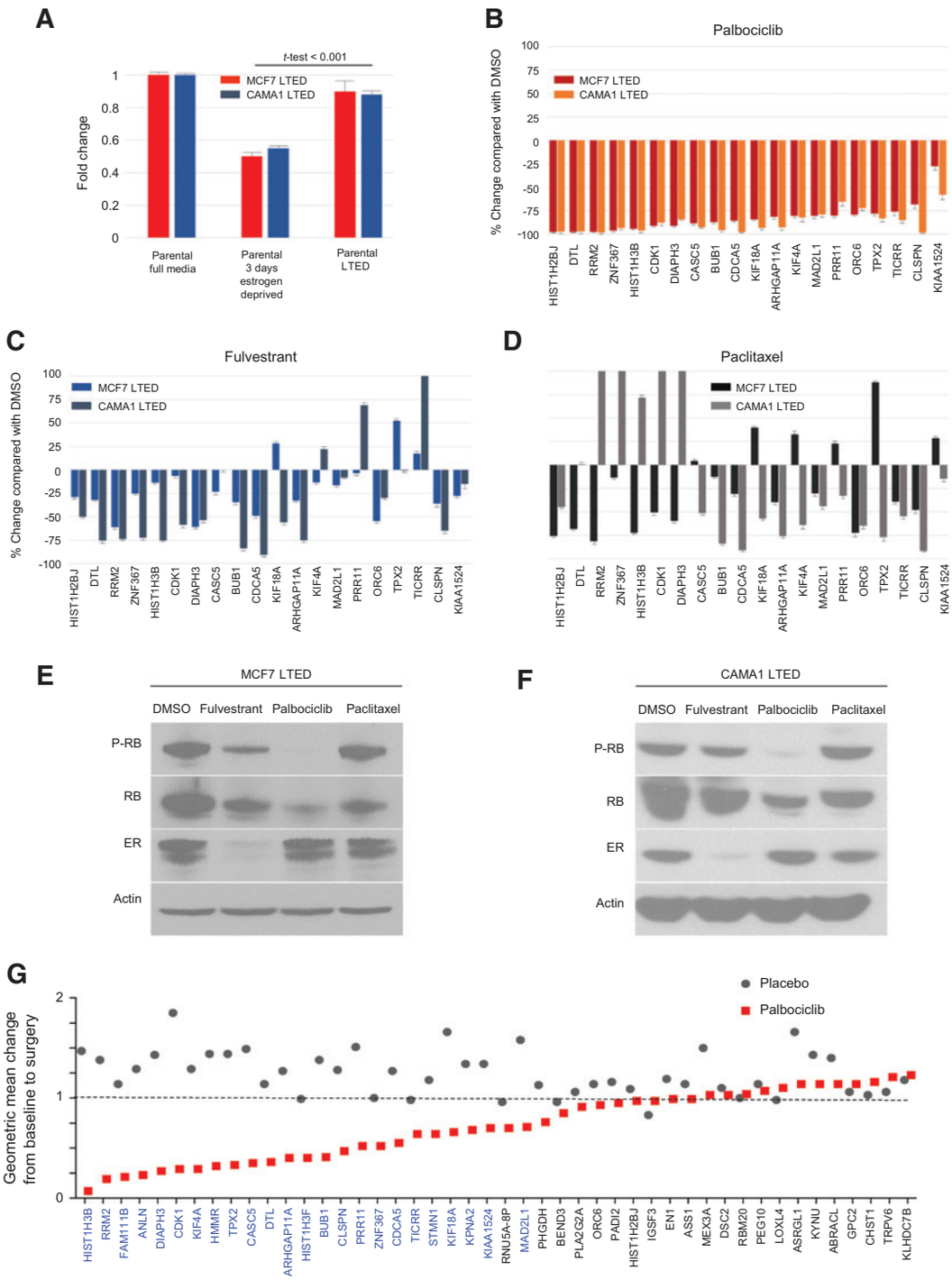

Figure 4.

An E2F4 transcriptional program is associated with estrogen-independent proliferation in letrozole-resistant tumors and is modulated by CDK4/6 inhibitors. **A,** The expression levels of 20 E2F4-regulated genes overexpressed in nonresponder tumors were assessed by RT-PCR in MCF7 and CAMA1 LTED cells and normalized to their expression in MCF7 and CAMA1 parental cells, respectively. Data are presented as the 20 genes mean fold change ± SEM. **B,** Expression levels of the same 20 genes were assessed by RT-PCR in MCF7/LTED and CAMA1/LTED cells after treatment with palbociclib 1 μmol/L for 24 hours. **C** and **D,** Fulvestrant 1 μmol/L for 24 hours (**C**) or paclitaxel 20 nmol/L for 24 hours (**D**). Data are presented as mean percent change ± SEM relative to treatment with DMSO of two independent replicates. **E** and **F,** Immunoblots of lysates from MCF7/LTED (**E**) or CAMA1/LTED cells (**F**) treated with DMSO, fulvestrant 1 μmol/L, palbociclib 1 μmol/L, or paclitaxel 20 nmol/L for 24 hours. **G,** The geometric mean change, between baseline and surgery, for the top 47 genes associated with letrozole resistance in the study cohort, was assessed in tumor samples from 60 $ER^+/HER2^-$ primary tumors treated with placebo or palbociclib for 15 days in the POP trial (NCT02008734); in blue text are genes predicted to be E2F4 targets.

Downloaded from http://aacrjournals.org/clincancerres/article-pdf/24/11/2517/2045372/2517.pdf by KMLA - Hanyang University user on 23 June 2022

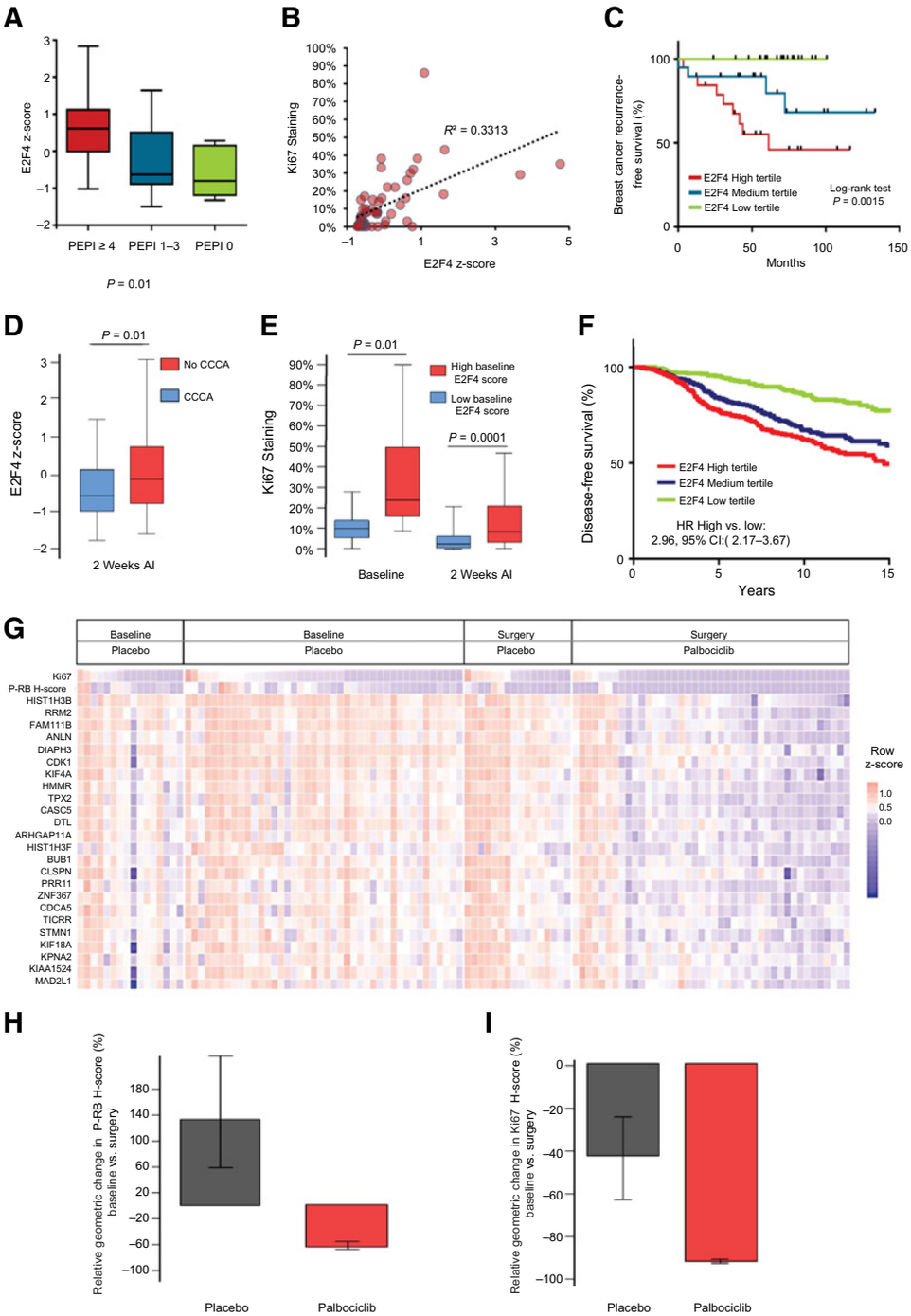

Figure 5.

An E2F4 target gene signature is associated with resistance to neoadjuvant and adjuvant endocrine therapy. **A–C,** An E2F4 activation signature was enriched in tumors with PEPI ≥4 (**A**), correlated with posttreatment Ki67 levels (**B**), and was associated with increased risk of breast cancer recurrence in the cohort of patients treated with prolonged neoadjuvant letrozole (**C**; Fig. 1). **D,** Box plots comparing the E2F4 signature score in ER$^+$/HER2$^-$ tumors from patients in the ACOSOG Z1031B study ($n = 110$, NCT01953588) after treatment with an AI. According to the 2-week Ki67 score, tumors were classified as achieving complete cell arrest (CCCA, Ki67 ≤ 2.7%) or no-CCCA (Ki67 > 2.7%), *P* value for *t* test. **E,** Box plot correlating high versus low E2F4 signature score with the Ki67 score at baseline and after 2 weeks of treatment with an AI in tumors from the ACOSOG Z1031B study. Tumors with a high E2F4 score at baseline exhibited a lower rate of CCCA upon treatment compared with tumors with a low baseline E2F4 score (18% vs. 50%), *P* value for *t* test. **F,** Disease-free survival in patients with ER$^+$ breast cancer treated with adjuvant endocrine therapy in the METABRIC database ($n = 1{,}498$) according to E2F4 signature score tertiles. **G,** Tile plot showing baseline and surgery gene expression values for each of the components of the E2F4 gene signature, Ki67, and P-RB score from 60 ER$^+$/HER2$^-$ tumors treated in the POP trial with either placebo or 2 weeks of palbociclib. **H** and **I,** Geometric mean change (±SD) in P-RB H-score (**H**) and Ki67 score (**I**) in 30 ER$^+$/HER2$^-$ tumor pairs before and after a 2-week treatment with placebo or palbociclib. Tumors are those with a high baseline E2F4 score.

Downloaded from http://aacrjournals.org/clincancerres/article-pdf/24/11/2517/2045372/2517.pdf by KMLA - Hanyang University user on 23 June 2022

tumors expressing high levels of E2F4 signature activity ($n = 30$), treatment with the CDK4/6 inhibitor was able to suppress P-RB by 90% but Ki67 by only 67% (Fig. 5H and I). We speculate that the partial suppression of Ki67 despite almost complete inhibition of P-RB could be accounted for by the lack of simultaneous antiestrogen therapy. In summary, we have identified a CDK4/6 inhibitor-sensitive E2F4 activation signature that defines ER^+ breast cancers with poor prognostic features. This signature is of potential use for the identification of patients with ER^+ breast cancer candidates for adjuvant therapy with CDK4/6 inhibitors in combination with antiestrogens.

Discussion

Neoadjuvant endocrine therapy trials offer an opportunity to discover functional genomic alterations associated with drug resistance that may inform postoperative adjuvant treatment. In this study, we performed targeted DNA and whole transcriptome sequencing in residual ER^+ breast cancers treated with letrozole for a median of 7.2 months. A higher number of mutations were found in patients with a poor response to estrogen deprivation with letrozole, confirming other studies (4, 8), and also suggesting a source of genetic diversity that may identify cancers that recur after adjuvant endocrine therapy. In agreement with other studies (33), we detected a different composition of intrinsic molecular subtypes to what would be expected in a cohort of untreated ER^+ postmenopausal breast cancers. The increase in tumors with a normal subtype and reduction in Luminal A tumors suggest a change induced by treatment, whereas the increase in tumors of the basal-like subtype suggests a loss of luminal expression and the outgrowth of endocrine-resistant cancer cell subpopulations.

We did not detect recurrent mutations or CNAs significantly enriched in tumors resistant to letrozole. However, there was a numerical increase in few clinically actionable mutations, such as *NF1* loss and in genes like *JAK1*, *NOTCH1*, *FGFR4*, and *PTPRD*, whose role in endocrine resistance has not yet been elucidated. We found a greater number of mutations in the PI3K pathway (*PIK3CA*, *AKT1*, *TSC2*, and/or loss or truncation mutations of *PTEN*) associated with poor response to letrozole, but only those PI3K pathway mutations in Luminal B/HER2–enriched/basal tumors were associated with poor features (high PEPI score, high proliferation, and breast cancer relapse). By applying a comprehensive set of breast cancer–related gene signatures, we showed that multiple pathways are involved in evading estrogen deprivation, including gene signatures related to growth factor receptor, RAS and PI3K signaling, and cancer cell stemness. Different to some prior reports (34), we did not observe an enrichment in immune-related gene expression signatures.

Integration of the 47 most upregulated genes in letrozole-resistant tumors with transcription-binding data identified a set of genes controlled by the E2F4 transcription factor. Consistent with activation of E2F4 by cyclin D/CDK4/6 complexes, treatment with the CDK4/6 inhibitor palbociclib downregulated this set of genes in primary ER^+ breast cancers simultaneous with a reduction in P-RB levels and tumor cell proliferation measured by Ki67 IHC. In the initial cohort of tumors treated with prolonged neoadjuvant letrozole (Fig. 1), the prognostic ability of this set of genes was independent of adjuvant chemotherapy, suggesting they may also be causal to chemotherapy resistance. In line with this hypothesis, paclitaxel was not able to suppress this set of genes *in vivo*. We found a marked upregulation of the E2F4 gene expression signature in AI-resistant tumors from patients in the ACOSOG Z1031B study. Of note, the endocrine-resistant tumors in ACOSOG Z1031B were also resistant to neoadjuvant chemotherapy, and several of the genes that compose the signature (i.e., *KIF4A*, *KIF18A*, *DIAPH3*, *TPX2*) have been causally associated with resistance to chemotherapy (35–37). Taken together, these data suggest CDK4/6 inhibitors would be an excellent therapeutic strategy against ER^+ breast cancers where antiestrogens do not inhibit tumor cell proliferation and/or other pharmacodynamic surrogates like the E2F4 score described herein. Two recent studies support this notion. First, the NEO-MONARCH trial showed an overall striking reduction in tumor cell proliferation (Ki67 score) in primary ER^+ breast cancers treated with the CDK4/6 inhibitor abemaciclib alone or in combination with letrozole (38). In a second example, Ma and collegues (39) treated patients with ER^+ breast cancer with the AI anastrozole for 28 days, at which time the Ki67 score was measured in a research biopsy and palbociclib was added. Complete cell-cycle arrest rate was significantly higher after adding palbociclib to anastrozole, suggesting that the addition of a CDK4/6 inhibitor can induce a more complete antiproliferative effect in tumors that exhibit partial growth suppression upon estrogen deprivation.

The role of E2F in endocrine resistance has been previously documented by our group (40) and others (41). Our results agree with studies that have shown the prognostic value of an E2F4 signature in ER^+ breast cancer (42). This signature, based on 199 E2F4 target genes, identified by *in vitro* ChIP-seq experiments, remains a significant prognostic factor in the adjuvant setting even after adjusting for clinicopathologic variables and adjuvant therapy (endocrine and/or chemotherapy). The finding that current adjuvant treatments cannot improve the prognosis of patients exhibiting high expression of this E2F4 signature also agrees with our results that only CDK4/6 inhibition, and not chemotherapy nor fulvestrant, is able to suppress completely E2F4 target gene expression. However, the same authors reported that high levels of the 199-gene E2F4 signature are predictive of pathologic complete response to neoadjuvant chemotherapy in ER^+ breast cancer (43). Although this might seem contradictory, transcriptional activity of E2F4 is a marker of highly proliferative tumors, which is a recognized predictive factor of an initial response to chemotherapy. However, if a tumor does not respond to preoperative endocrine therapy or chemotherapy, it is also known that high proliferation (measured by Ki67) is a marker of poor prognosis (44). Thus, we believe that a pharmacodynamic assessment of proliferation, particularly in ER^+ tumors, can clearly unmask highly proliferative tumors with a poor prognosis. Our E2F4 signature differs from the E2F4 signature mentioned above mainly on the biological and clinical contexts from which it is derived. Instead of *in vitro* data, we used on-treatment primary tumor data from a cohort of patients with ER^+ breast cancer treated preoperatively with standard-of-care letrozole. Therefore, we believe that the established biology of our signature and the context of its discovery may facilitate its implementation in neoadjuvant endocrine studies testing the performance of new drugs.

Some limitations of the current study are the lack of baseline DNA/RNA-seq data that precluded direct comparisons between untreated and on-treatment samples. Thus, we used TCGA data as baseline. Indirect comparisons of genetic alterations among studies can be subjected to bias regarding software pipeline, sequencing depth, and tumor content. Also, the disproportion in sample

Downloaded from http://aacrjournals.org/clincancerres/article-pdf/24/11/2517/2045372/2517.pdf by KMLA - Hanyang University user on 23 June 2022

size and some particularities between the two datasets, such as age, might account for some of the differences we found.

In conclusion, we have identified genomic alterations and transcriptional phenotypes in a cohort of $ER^+/HER2^-$ breast cancers resistant to prolonged estrogen deprivation. Results suggest the presence of an ER-independent E2F4 gene expression program that can be blocked by inhibition of CDK4/6. We posit these tumors may require combined inhibition of ER and CDK4/6 for a maximal anticancer effect.

Disclosure of Potential Conflicts of Interest

J.M. Giltnane is an employee of Genentech. J. Gavilá reports receiving speakers bureau honoraria from Novartis and Roche and is a consultant/advisory board member for Novartis. F. Andre is a consultant/advisory board member for Lilly, Novartis, and Pfizer. M. Arnedos reports receiving commercial research grants from Lilly, speakers bureau honoraria from AstraZeneca and Novartis, and is a consultant/advisory board member for Seattle Genetics. C.L. Arteaga is a member of an advisory board for Novartis and a member of the scientific advisory board for the Komen Foundation. No potential conflicts of interest were disclosed by the other authors.

Authors' Contributions

Conception and design: A.L. Guerrero-Zotano, T.P. Stricker, C.L. Arteaga
Development of methodology: A.L. Guerrero-Zotano, J.M. Giltnane, C.L. Arteaga
Acquisition of data (provided animals, acquired and managed patients, provided facilities, etc.): A.L. Guerrero-Zotano, L. Formisano, K.-M. Lee, L.J. Schwarz, M.V. Estrada, V.M. Jansen, A. Servetto, J. Gavilá, J.A. Perez-Fidalgo, A. Lluch, A. Llombart-Cussac, M.A. Bayar, S. Michiels, F. André, M. Arnedos, V. Guillem, A. Ruiz-Simon, C.L. Arteaga
Analysis and interpretation of data (e.g., statistical analysis, biostatistics, computational analysis): A.L. Guerrero-Zotano, T.P. Stricker, L. Formisano, K.E. Hutchinson, D.G. Stover, L.J. Schwarz, M.V. Estrada, A. Llombart-Cussac, M.A. Bayar, S. Michiels, F. André, C.L. Arteaga
Writing, review, and/or revision of the manuscript: A.L. Guerrero-Zotano, T.P. Stricker, K.E. Hutchinson, D.G. Stover, L.J. Schwarz, J.M. Giltnane, V.M. Jansen, J. Gavilá, J.A. Perez-Fidalgo, A. Lluch, M.A. Bayar, S. Michiels, F. André, M. Arnedos, V. Guillem, A. Ruiz-Simon, C.L. Arteaga
Administrative, technical, or material support (i.e., reporting or organizing data, constructing databases): A.L. Guerrero-Zotano, J.M. Giltnane, J. Gavilá, M.A. Bayar, C.L. Arteaga
Study supervision: A.L. Guerrero-Zotano, C.L. Arteaga

Acknowledgments

This study was supported by NIH Breast SPORE grant P50 CA098131, Vanderbilt-Ingram Cancer Center Support grant P30 CA68485, Susan G. Komen for the Cure Breast Cancer Foundation grant SAC100013, a grant from the Breast Cancer Research Foundation, a grant from the Sociedad Española de Oncología Médica (SEOM), a grant from the Asociación Española Contra el Cáncer (AECC), and a grant from Grupo Español de Investigación en Cáncer de Mama (GEICAM).

The costs of publication of this article were defrayed in part by the payment of page charges. This article must therefore be hereby marked *advertisement* in accordance with 18 U.S.C. Section 1734 solely to indicate this fact.

Received October 4, 2017; revised February 9, 2018; accepted March 20, 2018; published first March 26, 2018.

References

1. Kohler BA, Sherman RL, Howlader N, Jemal A, Ryerson AB, Henry KA, et al. Annual report to the nation on the status of cancer, 1975-2011, featuring incidence of breast cancer subtypes by race/ethnicity, poverty, and state. J Natl Cancer Inst 2015;107:djv048.
2. Cuzick J, Sestak I, Baum M, Buzdar A, Howell A, Dowsett M, et al. Effect of anastrozole and tamoxifen as adjuvant treatment for early-stage breast cancer: 10-year analysis of the ATAC trial. Lancet Oncol 2010;11:1135–41.
3. Early Breast Cancer Trialists' Collaborative Group (EBCTCG). Aromatase inhibitors versus tamoxifen in early breast cancer: patient-level meta-analysis of the randomised trials. Lancet 2015;386:1341–52.
4. Ellis MJ, Ding L, Shen D, Luo J, Suman VJ, Wallis JW, et al. Whole-genome analysis informs breast cancer response to aromatase inhibition. Nature 2012;486:353–60.
5. Dowsett M, Smith IE, Ebbs SR, Dixon JM, Skene A, Griffith C, et al. Short-term changes in Ki-67 during neoadjuvant treatment of primary breast cancer with anastrozole or tamoxifen alone or combined correlate with recurrence-free survival. Clin Cancer Res 2005;11:951s–8s.
6. Ellis MJ, Coop A, Singh B, Tao Y, Llombart-Cussac A, Jänicke F, et al. Letrozole inhibits tumor proliferation more effectively than tamoxifen independent of HER1/2 expression status. Cancer Res 2003;63:6523–31.
7. Ellis MJ, Suman VJ, Hoog J, Goncalves R, Sanati S, Creighton CJ, et al. Ki67 proliferation index as a tool for chemotherapy decisions during and after neoadjuvant aromatase inhibitor treatment of breast cancer: results from the american college of surgeons oncology group Z1031 trial (Alliance). J Clin Oncol 2017;35:1061–69.
8. Gellert P, Segal CV, Gao Q, López-Knowles E, Martin L-A, Dodson A, et al. Impact of mutational profiles on response of primary oestrogen receptor-positive breast cancers to oestrogen deprivation. Nat Commun 2016;7:13294.
9. Miller CA, Gindin Y, Lu C, Griffith OL, Griffith M, Shen D, et al. Aromatase inhibition remodels the clonal architecture of estrogen-receptor-positive breast cancers. Nat Commun 2016;7:12498.
10. Creighton CJ, Li X, Landis M, Dixon JM, Neumeister VM, Sjolund A, et al. Residual breast cancers after conventional therapy display mesenchymal as well as tumor-initiating features. Proc Natl Acad Sci U S A 2009;106:13820–5.
11. Ellis MJ, Tao Y, Luo J, A'Hern R, Evans DB, Bhatnagar AS, et al. Outcome prediction for estrogen receptor-positive breast cancer based on postneoadjuvant endocrine therapy tumor characteristics. J Natl Cancer Inst 2008;100:1380–8.
12. Llombart-Cussac A, Guerrero Á, Galán A, Carañana V, Buch E, Rodríguez-Lescure Á, et al. Phase II trial with letrozole to maximum response as primary systemic therapy in postmenopausal patients with ER/PgR[+] operable breast cancer. Clin Transl Oncol 2012;14:125–31.
13. Eisenhauer EA, Therasse P, Bogaerts J, Schwartz LH, Sargent D, Ford R, et al. New response evaluation criteria in solid tumours: revised RECIST guideline (version 1.1). Eur J Cancer 2009;45:228–47.
14. Allred DC, Harvey JM, Berardo M, Clark GM. Prognostic and predictive factors in breast cancer by immunohistochemical analysis. Mod Pathol 1998;11:155–68.
15. McKenna A, Hanna M, Banks E, Sivachenko A, Cibulskis K, Kernytsky A, et al. The genome analysis toolkit: a MapReduce framework for analyzing next-generation DNA sequencing data. Genome Res 2010;20:1297–303.
16. Wang K, Li M, Hakonarson H. ANNOVAR: functional annotation of genetic variants from high-throughput sequencing data. Nucleic Acids Res 2010;38:e164.
17. Lek M, Karczewski KJ, Minikel EV, Samocha KE, Banks E, Fennell T, et al. Analysis of protein-coding genetic variation in 60,706 humans. Nature 2016;536:285–91.
18. Ng PC, Henikoff S. SIFT: predicting amino acid changes that affect protein function. Nucleic Acids Res 2003;31:3812–4.
19. Davydov EV, Goode DL, Sirota M, Cooper GM, Sidow A, Batzoglou S. Identifying a high fraction of the human genome to be under selective constraint using GERP++. PLOS Computat Biol 2010;6:e1001025.
20. Adzhubei IA, Schmidt S, Peshkin L, Ramensky VE, Gerasimova A, Bork P, et al. A method and server for predicting damaging missense mutations. Nat Methods 2010;7:248–9.
21. Tamborero D, Rubio-Perez C, Deu-Pons J, Schroeder MP, Vivancos A, Rovira A, et al. Cancer Genome Interpreter annotates the biological and clinical relevance of tumor alterations. Genome Med 2018;10:25.
22. Love MI, Huber W, Anders S. Moderated estimation of fold change and dispersion for RNA-seq data with DESeq2. Genome Biol 2014;15:550.

Downloaded from http://aacrjournals.org/clincancerres/article-pdf/24/11/2517/2045372/2517.pdf by KMLA - Hanyang University user on 23 June 2022

23. Stover DG, Coloff JL, Barry WT, Brugge JS, Winer EP, Selfors LM. The role of proliferation in determining response to neoadjuvant chemotherapy in breast cancer: a gene expression-based meta-analysis. Clin Cancer Res 2016;22:6039–50.
24. Parker JS, Mullins M, Cheang MCU, Leung S, Voduc D, Vickery T, et al. Supervised risk predictor of breast cancer based on intrinsic subtypes. J Clin Oncol 2009;27:1160–7.
25. Jiang T, Shi W, Natowicz R, Ononye SN, Wali VB, Kluger Y, et al. Statistical measures of transcriptional diversity capture genomic heterogeneity of cancer. BMC Genomics 2014;15:876.
26. Ciriello G, Gatza ML, Beck AH, Wilkerson MD, Rhie SK, Pastore A, et al. Comprehensive molecular portraits of invasive lobular breast cancer. Cell 2015;163:506–19.
27. Curtis C, Shah SP, Chin S-F, Turashvili G, Rueda OM, Dunning MJ, et al. The genomic and transcriptomic architecture of 2,000 breast tumours reveals novel subgroups. Nature 2012;486:346–52.
28. Miller TW, Hennessy BT, González-Angulo AM, Fox EM, Mills GB, Chen H, et al. Hyperactivation of phosphatidylinositol-3 kinase promotes escape from hormone dependence in estrogen receptor–positive human breast cancer. J Clin Invest 2010;120:2406–13.
29. Schiavon G, Hrebien S, Garcia-Murillas I, Cutts RJ, Pearson A, Tarazona N, et al. Analysis of ESR1 mutation in circulating tumor DNA demonstrates evolution during therapy for metastatic breast cancer. Sci Transl Med 2015;7:313ra182.
30. Kuleshov MV, Jones MR, Rouillard AD, Fernandez NF, Duan Q, Wang Z, et al. Enrichr: a comprehensive gene set enrichment analysis web server 2016 update. Nucleic Acids Res 2016;44:W90–7.
31. Lindeman GJ, Gaubatz S, Livingston DM, Ginsberg D. The subcellular localization of E2F-4 is cell-cycle dependent. PNAS 1997;94:5095–100.
32. Arnedos M, Cheaib B, Bayar MA, Michiels S, Scott V, Adam J, et al. Abstract CT041: Anti-proliferative response and predictive biomarkers to palbociclib in early breast cancer: the preoperative palbociclib (POP) randomized trial. Cancer Res 2016;76:CT041.
33. Dunbier AK, Anderson H, Ghazoui Z, Salter J, Parker JS, Perou CM, et al. Association between breast cancer subtypes and response to neoadjuvant anastrozole. Steroids 2011;76:736–40.
34. Turnbull AK, Arthur LM, Renshaw L, Larionov AA, Kay C, Dunbier AK, et al. Accurate prediction and validation of response to endocrine therapy in breast cancer. J Clin Oncol 2015;33:2270–8.
35. Tilghman J, Wu H, Sang Y, Shi X, Guerrero-Cazares H, Quinones-Hinojosa A, et al. HMMR maintains the stemness and tumorigenicity of glioblastoma stem-like cells. Cancer Res 2014;74:3168–79.
36. Warner SL, Stephens BJ, Nwokenkwo S, Hostetter G, Sugeng A, Hidalgo M, et al. Validation of TPX2 as a potential therapeutic target in pancreatic cancer cells. Clin Cancer Res 2009;15:6519–28.
37. Tan MH, De S, Bebek G, Orloff MS, Wesolowski R, Downs-Kelly E, et al. Specific kinesin expression profiles associated with taxane resistance in basal-like breast cancer. Breast Cancer Res Treat 2012; 131:849–58.
38. Hurvitz S, Abad MF, Rostorfer R, Chan D, Egle D, Huang C-S, et al. breast cancer, early stageInterim results from neoMONARCH: a neoadjuvant phase II study of abemaciclib in postmenopausal women with HR + /HER2- breast cancer (BC). Ann Oncol 2016;27:LBA13.
39. Ma CX, Gao F, Luo J, Northfelt DW, Goetz MP, Forero A, et al. NeoPalAna: neoadjuvant palbociclib, a cyclin-dependent kinase 4/6 inhibitor, and anastrozole for clinical stage 2 or 3 estrogen receptor positive breast cancer. Clin Cancer Res 2017;23:4055–65.
40. Miller TW, Balko JM, Fox EM, Ghazoui Z, Dunbier A, Anderson H, et al. ERα-dependent E2F transcription can mediate resistance to estrogen deprivation in human breast cancer. Cancer Discov 2011;1:338–51.
41. Chu J, Zhu Y, Liu Y, Sun L, Lv X, Wu Y, et al. E2F7 overexpression leads to tamoxifen resistance in breast cancer cells by competing with E2F1 at miR-15a/16 promoter. Oncotarget 2015;6:31944–57.
42. Khaleel SS, Andrews EH, Ung M, DiRenzo J, Cheng C. E2F4 regulatory program predicts patient survival prognosis in breast cancer. Breast Cancer Res 2014;16:486.
43. Mark KMK, Varn FS, Ung MH, Qian F, Cheng C. The E2F4 prognostic signature predicts pathological response to neoadjuvant chemotherapy in breast cancer patients. BMC Cancer 2017;17:306.
44. Denkert C, Budczies J, von Minckwitz G, Wienert S, Loibl S, Klauschen F. Strategies for developing Ki67 as a useful biomarker in breast cancer. Breast 2015;24:S67–72.

Downloaded from http://aacrjournals.org/clincancerres/article-pdf/24/11/2517/2045372/2517.pdf by KMLA - Hanyang University user on 23 June 2022